Preprint
UCRL-JC-148874

# Solving the Radiation Diffusion and Energy Balance Equations Using Pseudo Transient Continuation

*A.I. Shestakov and J.H. Bolstad*

*This paper will be part of Proceedings for the Nuclear Explosives Code Developers Conference held October 21-24, 2002.*

**U.S. Department of Energy**

Lawrence
Livermore
National
Laboratory

**February 1, 2002**

Approved for public release; further dissemination unlimited

## DISCLAIMER

This document was prepared as an account of work sponsored by an agency of the United States Government. Neither the United States Government nor the University of California nor any of their employees, makes any warranty, express or implied, or assumes any legal liability or responsibility for the accuracy, completeness, or usefulness of any information, apparatus, product, or process disclosed, or represents that its use would not infringe privately owned rights. Reference herein to any specific commercial product, process, or service by trade name, trademark, manufacturer, or otherwise, does not necessarily constitute or imply its endorsement, recommendation, or favoring by the United States Government or the University of California. The views and opinions of authors expressed herein do not necessarily state or reflect those of the United States Government or the University of California, and shall not be used for advertising or product endorsement purposes.

This is a preprint of a paper intended for publication in a journal or proceedings. Since changes may be made before publication, this preprint is made available with the understanding that it will not be cited or reproduced without the permission of the author.

# An exact solution for the linearized multifrequency radiation diffusion equation (U)

**A. I. Shestakov and J. H. Bolstad**

Lawrence Livermore National Laboratory

*An exact solution, based on Fourier and Laplace (FL) transforms, is developed for a linearization of the system modeling the multifrequency radiation diffusion and matter energy balance equations. The model uses an ideal gas equation of state. Opacities are proportional to the inverse of the cube of the frequency, thereby simulating free-free transitions. The solution is obtained in terms of integrals over the FL coefficients of the initial conditions and explicit sources. Results are presented for two special cases. (1) No sources, initially cold radiation field, and a localized matter energy profile. (2) Initially cold matter and radiation fields and a source of matter energy extending over finite space and time intervals. (U)*

## 1. Linear test problem

We present a solution for a linearized system modeling multifrequency radiation diffusion. We begin with the nondimensional multifrequency radiation diffusion equations derived by Hald and Shestakov (H&S) [1] to which we add explicit sources $\mathcal{S}$. If the frequency coordinate is discretized into $N$ groups,

$$0 = \nu_0 < \nu_1 < \ldots < \nu_N \,,$$

and the H&S equations are integrated over the frequency intervals, see [2], one obtains the following system of $N+1$ equations coupling the $N$ radiation energy densities $w_j$, $j = 1, \ldots, N$, to the matter temperature $T$,

$$\partial_t w_j = \mu_j \partial_{xx} w_j + p_j T - w_j/\mu_j + \mathcal{S}_j \,, \qquad [1]$$

$$R\,\partial_t T = -T + \sum_{j=1}^{N} w_j/\mu_j + \mathcal{S}_T \,. \qquad [2]$$

Equation (1) represents $N$ equations; each simulating the transport of the radiation in the $j$–th group. In (1)–(2), $\mu_j = \bar{\nu}_j^3$, where $\bar{\nu}_j$ is a group's representative frequency, satisfying

$$\nu_{j-1} < \bar{\nu}_j < \nu_j \,.$$

Equation (1) shows that $w_j$ diffuses with a diffusion coefficient $\mu_j$. Additionally, $w_j$ undergoes absorption at the rate $\mu_j^{-1}$ while $p_j T$ is the rate of energy that the $j$th group receives from the matter. The emission coefficient

$$p_j \doteq \exp(-\nu_{j-1}/T) - \exp(-\nu_j/T) \qquad [3]$$

and $R$, which plays the role of the heat capacity, is a positive constant. In the limit of small group widths,

$$p_j = \exp(-\nu_{j-1}/T)\,(\delta_j - \delta_j^2/2 + \dots)\,, \qquad [4]$$

where $\delta_j = (\nu_j - \nu_{j-1})/T$. The mesh $\{\,\nu_j\,\}$ is assumed to be sufficiently broad so that for all relevant $T$,

$$\nu_1 \ll T \ll \nu_N\,,$$

which implies

$$\sum_{j=1}^{N} p_j = 1\,. \qquad [5]$$

To be precise, the broadness requirement of the mesh $\{\nu_j\}$ is

$$1/\mu_N \approx 1/\nu_N^3 \approx 0\,.$$

Thus, even if we had energy at $\nu > \nu_N$, it is irrelevant for our purposes since that high frequency radiation would not be absorbed by the matter; thus, does not interact with the model.

Although (1)–(2) are in nondimensional form, to avoid confusion, we note that $w_j$ is the analogue of the radiation energy density per frequency *multiplied by* the group width. Hence, $\sum_j w_j$ represents the radiation energy density.

In this paper, in order to obtain a tractable linear system, we assume that the temperature used to define $p_j$, see (3), is set to a constant value $T_0$. That is,

$$p_j = p_j(T_0)\,.$$

The restriction *only* applies to (3).[1]. The system of interest, (1)–(2), consists of $N+1$ evolution equations, $N$ equations for the $w_j$ and one for $T$.

At this point, it is worthwhile to discuss the implication of the linearization. That is, to compare the difference between using (3) as it stands or using $T_0$ to define $p_j$. For a sufficiently fine frequency grid, (4) implies that in the original (nonlinear) H&S model, radiation is emitted into the $j^{\text{th}}$ group at the rate $\exp(-\nu_j/T)\,(\nu_j - \nu_{j-1})$. In our linearized system, radiation is emitted at the rate $p_j(T_0)\,T$. If $T \approx T_0$ throughout the simulation, the emission is approximately the same; hence, so are solutions to the linear and nonlinear systems. The difference between the linear and nonlinear systems is illustrated in Fig. 1 where we plot $p_j$ for various $T$. For example, assume that in a problem $T$ ranges from 0.1 to 10.0, but we use $T = 1$ to define $p_j$. Thus our linearized model, when it converts matter energy into the radiation field, preferentially puts it into groups 35–55 rather than groups 15–30 where $T \approx 0.1$ and groups 60–80 where $T \approx 10$.

The advantage of the linearized equations is that we can obtain solutions in closed form. Our approach follows that of Su and Olson [3] and [4]. The problem is attacked using Fourier transforms in space and Laplace transforms in time. For a function $f(x,t)$, if

$$\hat{f}_{k,s} \doteq \int_0^\infty dt\, e^{-st} \int_{-\infty}^{\infty} dx\, f(x,t)\, e^{ikx}, \qquad (\,i = \sqrt{-1})$$

[1] It also applies to (4) where now $\delta_j = (\nu_j - \nu_{j-1})/T_0$

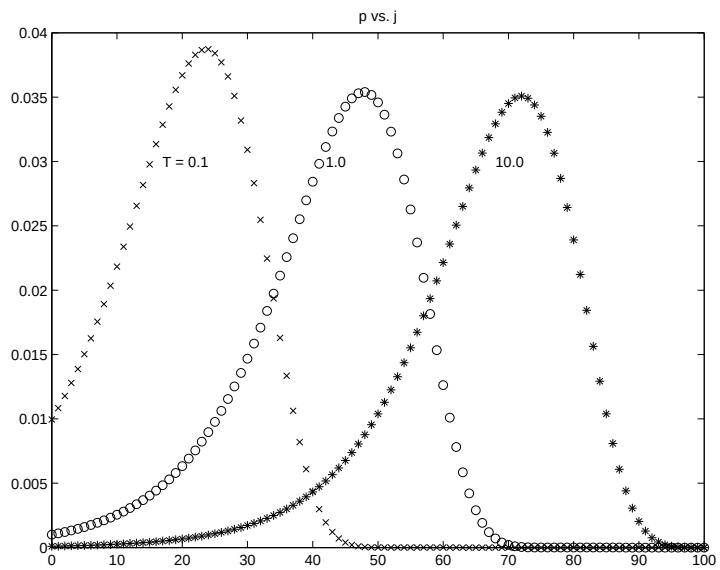


Fig. 1. Emission coefficient $p_j$ vs. $j$ for various $T$. Frequency width: $\nu_1 = 10^{-3}$, $\nu_{j+1} - \nu_j = 1.1\,(\,\nu_j - \nu_{j-1}\,)$ .

defines the transform of $f$, (1)–(2) transform into

$$\begin{aligned} -\hat{w}_{j,k} + s\,\hat{w}_{j,k,s} &= -k^2\,\mu_j\,\hat{w}_{j,k,s} + p_j\,\hat{T}_{k,s} - \hat{w}_{j,k,s}/\mu_j + \hat{\mathcal{S}}_{j,k,s} \\ -R\,\hat{T}_k + R\,s\,\hat{T}_{k,s} &= -\hat{T}_{k,s} + \sum_{j=1}^{N} \hat{w}_{j,k,s}/\mu_j + \hat{\mathcal{S}}_{T,k,s}\,, \end{aligned}$$

where $\hat{w}_{j,k}$ and $\hat{T}_k$, the harmonics of the initial conditions, do not depend on $s$. Rearranging terms and combining the initial conditions with the sources yields the transformed linear system

$$\hat{w}_{j,k,s}\,/(\mu_j\,\gamma_{j,k,s}) - p_j\,\hat{T}_{k,s} = \hat{\Sigma}_{j,k,s} \qquad (j = 1,\,\ldots\,,\,N), \qquad [6]$$

$$-\sum_{j=1}^{N} \hat{w}_{j,k,s}/\mu_j + (1 + R\,s)\,\hat{T}_{k,s} = \hat{\Sigma}_{T,k,s}, \qquad [7]$$

where

$$\gamma_{j,k,s} = 1/(1 + s\,\mu_j + k^2\mu_j^2) \qquad [8]$$

and

$$\hat{\Sigma}_{j,k,s} = \hat{w}_{j,k} + \hat{\mathcal{S}}_{j,k,s} \;\;,\;\; \hat{\Sigma}_{T,k,s} = R\,\hat{T}_k + \hat{\mathcal{S}}_{T,k,s}\,.$$

The explicit sources play the same role as the initial conditions.

The system (6)–(7) can be solved explicitly.[2] We obtain

$$\hat{T}_{k,s} = \frac{1}{d_{k,s}}\left(\hat{\Sigma}_{T,k,s} + \sum_{\ell=1}^{N} \gamma_{\ell,k,s}\,\hat{\Sigma}_{\ell,k,s}\right) \qquad [9]$$

[2]Solve (6) for $\hat{w}_{j,k,s}$ and substitute the result into (7). Solving for $\hat{T}_{k,s}$ yields (9); substituting the result into (6) yields (10).

$$\hat{w}_{j,k,s} \;=\; \frac{p_j\,\mu_j\,\gamma_{j,k,s}}{d_{k,s}}\left(\hat{\Sigma}_{T,k,s}+\frac{d_{k,s}}{p_j}\,\hat{\Sigma}_{j,k,s}+\sum_{\ell=1}^{N}\gamma_{\ell,k,s}\,\hat{\Sigma}_{\ell,k,s}\right), \qquad [10]$$

where

$$d_{k,s}=1+R\,s-\sum_{j=1}^{N}p_j\,\gamma_{j,k,s}=R\,s+\sum_{j=1}^{N}\frac{p_j\,(s\,\mu_j+k^2\mu_j^2)}{1+s\,\mu_j+k^2\mu_j^2}\,. \qquad [11]$$

The last equality is due to the definition of $\gamma_{j,k,s}$ and (5).

Once the harmonics are computed, the solution is given via the inverse transform

$$f(x,t)=\frac{1}{2\pi i}\int_{\zeta-i\infty}^{\zeta+i\infty}ds\,e^{st}\left(\frac{1}{2\pi}\int_{-\infty}^{+\infty}dk\,\hat{f}_{k,s}e^{-ikx}\right),$$

with $\zeta$ taken to the right of all the singularities in the complex $s$–plane.

In the following sections we consider two problems. Both are initialized with $w_j|_{t=0}=0$ and we discard explicit radiation sources, i.e., we set $\mathcal{S}_j=0$. In the first problem, $\mathcal{S}_T=0$ and we initialize $T$ with a localized profile. In the second problem, initially $T=0$, but we inject a pulse of localized energy into the matter. First we derive the analytical solutions, given as integrals over the harmonics. In the latter sections, we present numerical results, which we obtain by quadratures.

## 2. Initially localized matter energy

We consider a problem without sources, but with an initial condition consisting of matter energy localized in the region $|x|\le x_0$. Let $|x|<\infty$ define the domain and impose the boundary conditions,

$$\lim_{x\to\pm\infty}(\,w_j,T)=0\,.$$

For the initial condition, let

$$w_j|_{t=0}=\mathcal{S}_T=\mathcal{S}_j=0 \qquad (j=1,\,\ldots,\,N)\,,\quad \text{and}$$

$$T(x)|_{t=0}=H(x+x_0)-H(x-x_0),$$

where $H$ is the Heaviside function. This implies that the total energy is

$$E(t)\doteq\int_{-\infty}^{+\infty}dx\left(R\,T+\sum_{j=1}^{N}w_j\right)=\int_{-\infty}^{+\infty}dx\,R\,T(x)|_{t=0}=2\,R\,x_0\,. \qquad [12]$$

It follows that only the transform of $T(x)|_{t=0}$,

$$\hat{T}_k=2\sin(kx_0)/k\,,$$

contributes to the solution. The harmonics are given by

$$\hat{T}_{k,s} \;=\; \hat{\Sigma}_{T,k,s}/d_{k,s}\,, \qquad [13]$$

$$\hat{w}_{j,k,s} \;=\; p_j\,\mu_j\,\gamma_{j,k,s}\,\hat{\Sigma}_{T,k,s}/d_{k,s}\,, \qquad [14]$$

where

$$\hat{\Sigma}_{T,k,s} = R\hat{T}_k = 2\,R\,\sin(kx_0)/k\,.$$

In closed form,

$$T(x,t) = \frac{R}{2\pi^2 i}\int_{\zeta-i\infty}^{\zeta+i\infty} ds\, e^{st}\left(\int_{-\infty}^{+\infty} dk\, e^{-ikx}\,\frac{\sin(kx_0)}{k}\,\frac{1}{d_{k,s}}\right), \qquad [15]$$

where $d_{k,s}$ is defined in (11). We let $s = \zeta + i\omega$ with $\zeta > 0$ and expand (15) into real and imaginary parts.[3] After deleting odd terms which are integrated from $-\infty$ to $\infty$, we reduce (15) to

$$T(x,t) = \frac{2\,R\,e^{\zeta t}}{\pi^2}\int_0^\infty dk\,\cos(kx)\,\frac{\sin(kx_0)}{k}\times \int_0^\infty d\omega\,[\,\mathcal{A}'_{k,\omega}\,\cos(\omega t) + \omega\,\mathcal{B}'_{k,\omega}\,\sin(\omega t)], \qquad [16]$$

where

$$\mathcal{A}'_{k,\omega} = \frac{\mathcal{A}_{k,\omega}}{\mathcal{A}^2_{k,\omega} + \omega^2\mathcal{B}^2_{k,\omega}}\,, \quad \mathcal{B}'_{k,\omega} = \frac{\mathcal{B}_{k,\omega}}{\mathcal{A}^2_{k,\omega} + \omega^2\mathcal{B}^2_{k,\omega}}\,, \qquad [17]$$

$$\mathcal{A}_{k,\omega} = R\zeta + 1 - \sum_{j=1}^{N} p_j\,A_{j,k,\omega}\,, \quad \mathcal{B}_{k,\omega} = R + \sum_{j=1}^{N} p_j\,B_{j,k,\omega}\,, \qquad [18]$$

$$A_{j,k,\omega} = \frac{\gamma_{j,k,\zeta}}{1+\omega^2\mu_j^2\gamma^2_{j,k,\zeta}}, \text{ and } B_{j,k,\omega} = \frac{\mu_j\,\gamma^2_{j,k,\zeta}}{1+\omega^2\mu_j^2\gamma^2_{j,k,\zeta}}\,, \qquad [19]$$

where $\gamma_{j,k,\zeta}$ is defined in (8); note that in (19), $\zeta$ replaces $s$ in the subscript. The formula for $\mathcal{A}_{k,\omega}$ suffers from numerical cancellation when $k$, $\omega$ and $\zeta$ are small. Using (5), $\mathcal{A}_{k,\omega}$ may be written in the equivalent but numerically stable form

$$\mathcal{A}_{k,\omega} = R\zeta + \sum_{j=1}^{N} p_j\mu_j\,\frac{(\zeta + k^2\mu_j)\,\gamma_{j,k,\zeta} + \omega^2\mu_j\gamma^2_{j,k,\zeta}}{1+\omega^2\mu_j^2\gamma^2_{j,k,\zeta}}.$$

The energies $w_j$ are obtained by recalling the distinction between the harmonics — see (13), (14). We find

$$w_j(x,t) = p_j\mu_j\,\frac{2\,R\,e^{\zeta t}}{\pi^2}\int_0^\infty dk\,\cos(kx)\,\frac{\sin(kx_0)}{k}\times \int_0^\infty d\omega\,[\,\mathcal{A}''_{j,k,\omega}\cos(\omega t) + \omega\,\mathcal{B}''_{j,k,\omega}\sin(\omega t)]\,, \qquad [20]$$

where

$$\begin{aligned}\mathcal{A}''_{j,k,\omega} &= \mathcal{A}'_{k,\omega}\,A_{j,k,\omega} - \omega^2\,\mathcal{B}'_{k,\omega}\,B_{j,k,\omega},\\ \mathcal{B}''_{j,k,\omega} &= \mathcal{A}'_{k,\omega}\,B_{j,k,\omega} + \mathcal{B}'_{k,\omega}\,A_{j,k,\omega},\end{aligned}$$

[3] We cannot take $\zeta = 0$ since $d_{k,s}$ in our inner integrand produces a simple pole at $s = 0$ when $k = 0$. The denominators of $\mathcal{A}'_{k,\omega}$ and $\mathcal{B}'_{k,\omega}$ are nonnegative for $\zeta \geq 0$, so this is the only singularity in the right half $s$-plane.

and $\mathcal{A}'_{k,\omega}$, $A_{j,k,\omega}$, etc. are defined in (17)–(19).

## 3. Explicit matter energy source

We now consider a problem which simulates the decay of an explicit source. As before, let $|x| < \infty$ define the domain. Assume that initially both the matter and radiation field are cold and the radiation source is zero, i.e.,

$$T|_{t=0} = w_j|_{t=0} = \mathcal{S}_j = 0 \qquad (j = 1, \ldots, N).$$

And, into the matter, for $0 < t < t_0$ and $|x| < x_0$,

$$\mathcal{S}_T = \mathcal{S}_T(x,t) = [H(t) - H(t-t_0)]\,[H(x+x_0) - H(x-x_0)]\,,$$

where $H$ is the Heaviside function. Thus, the total energy is

$$\begin{aligned} E(t) &\doteq \int_{-\infty}^{+\infty} dx \left( RT + \sum_{j=1}^{N} w_j \right) \\ &= \int_0^t d\tau \int_{-x_0}^{+x_0} dx\, \mathcal{S}_T(x,\tau) = 2x_0 \min(t,\, t_0)\,. \end{aligned} \qquad [21]$$

With these conditions, only the transform of the source $\mathcal{S}_T$,

$$\hat{\Sigma}_{T,k,s} = 2\,(1 - e^{-st_0})\sin(kx_0)/ks,$$

contributes to the solution and the harmonics are given by (13) and (14).

In closed form, $T(x,t)$ is given by a double integral similar to (15), viz.,

$$T(x,t) = \frac{1}{2\pi^2 i} \int_{\zeta - i\infty}^{\zeta + i\infty} ds\, \frac{e^{st}\,(1 - e^{-st_0})}{s} \left( \int_{-\infty}^{+\infty} dk\, e^{-ikx}\, \frac{\sin(kx_0)}{k}\, \frac{1}{d_{k,s}} \right), \qquad [22]$$

where $d_{k,s}$ is defined in (11).

As in the previous section, we let $s = \zeta + i\omega$ with $\zeta > 0$ and expand (22) into real and imaginary parts.[4] Proceeding as before, we reduce (22) to

$$T(x,t) = \frac{2\,e^{\zeta t}}{\pi^2} \int_0^\infty dk\, \cos(kx)\, \frac{\sin(kx_0)}{k} \times \int_0^\infty d\omega\, [(\omega F - \zeta\, G)\, \mathcal{A}'_{k,\omega} + \omega(\zeta\, F + \omega\, G)\, \mathcal{B}'_{k,\omega}]/(\zeta^2 + \omega^2), \qquad [23]$$

where $\mathcal{A}'_{k,\omega}$ and $\mathcal{B}'_{k,\omega}$ are defined in (17), and

$$\begin{aligned} F &= \sin(\omega t) - e^{-\zeta t_0} \sin(\omega\,(t - t_0))\,, \\ G &= e^{-\zeta t_0} \cos(\omega\,(t_0 - t)) - \cos(\omega t)\,. \end{aligned}$$

[4] This time there is a double pole at $s = 0$ when $k = 0$, and it is the only singularity in the right half $s$-plane.

The expression for $w_j$ is obtained as in the previous section. We find,

$$w_j(x,t) = p_j \mu_j \frac{2\, e^{\zeta t}}{\pi^2} \int_0^\infty dk\, \cos(kx)\, \frac{\sin(kx_0)}{k} \times \\ \int_0^\infty d\omega\, [(\omega F - \zeta\, G)\, \mathcal{A}''_{j,k,\omega} + \omega(\zeta\, F + \omega\, G)\, \mathcal{B}''_{j,k,\omega}]/(\zeta^2 + \omega^2). \qquad [24]$$

## 4. Evaluation of integrals

In this section we make a few remarks about the how to evaluate the integrals that define the functions $T$ and $w_j$. First, we list desirable properties of a quadrature method. We assume smooth integrands.

- Most importantly, since our integrals involve trigonometric functions, a quadrature method tailored to Fourier integrals is more efficient (and accurate) than one designed to handle "arbitrary" integrands over infinite intervals.
- The method should be of high order. Let $p$ be the order of accuracy of the quadrature method. If an error tolerance $\delta$ is specified, then in one dimension the work required is proportional to $\delta^{-1/p}$. But in two dimensions it is proportional to $\delta^{-2/p}$. In practice, high order is achieved by using low order methods and applying some form of Richardson extrapolation.
- The method should be adaptive. Since the chief expense in most methods is the evaluation of the integrands, one wants to evaluate them only where needed. For integrating over infinite intervals, an added benefit of adaptivity is that the process automatically decides where to cut off the infinite tails. Without adaptivity, some method must be devised to estimate the error committed when replacing an infinite by a finite interval.
- The method should supply a (global) error estimate for the result. One needs to know whether the answer is accurate to two digits or seven. It is easy to obtain such estimates when Richardson extrapolation is used; the starting point is to note that the difference between the high and low order approximation provides a global error estimate for the low order approximation. (This is also how an adaptive method decides where to adapt.)

The Quadpack [5] routine `dqawfe` satisfies these criteria. Romberg's method (trapezoid rule plus repeated Richardson extrapolation) satisfies only the second criterion; while Simpson's rule satisfies none. The ratio of computing times (for the same accuracy) of Simpson's rule or Romberg's method to an appropriate use (described below) of `dqawfe` can easily be more than one thousand to one.

The routine `dqawfe` computes Fourier integrals, of the form

$$\int_a^\infty f(\omega) \begin{Bmatrix} \cos(\omega x) \\ \sin(\omega x) \end{Bmatrix} d\omega,$$

where $a$ is finite. In principle, the function $f$ can be arbitrary, but in practice, the most accurate[5] and efficient results are obtained when the oscillatory behavior is confined to the trigonometric function, i.e., when $f$ is non-oscillatory. The outer integrals of the expressions for the temperature $T$ and radiation energy densities $w_j$ do not satisfy this condition, but are easily rewritten to do so. In the outer integrands of (16), (20), (23), and (24) we use a product formula for trigonometric functions to replace $\cos(kx)\sin(kx_0)$ by

$$[\,\sin(k(x_0+x)) + \sin(k(x_0-x))\,]/2\,.$$

Each outer integral is now expressed as the sum of two integrals, each of which is in the desirable form.

In summary, for each problem (and for both the temperature and radiation energy density), we call `dqawfe` twice to evaluate the outer integral. For the first problem (for either $T$ or $w_j$), each outer call of `dqawfe` results in two (recursive) calls of itself to evaluate the inner integrals. For the second problem, each outer call of `dqawfe` results in four recursive calls to evaluate the inner integrals.

Quadpack does not support recursion since it was written in Fortran 77. We circumvent the difficulty by using Fortran 90 and in every Quadpack routine that we call, we replace the keyword `subroutine` with `recursive subroutine`.

## 5. Numerical results

In this section we exhibit two sets of results. First, we display the solutions as functions of $x$ at various $t$. Then, we examine convergence of the solutions as the number of groups is increased. Third, we show the temporal evolution of the solutions at a fixed spatial point.

We fix the extent of the sources, by setting $x_0 = 1/2$ and $t_0 = 1$. We set the largest number of groups as $N = 64$ and specify the finest frequency grid as a geometric progression

$$\nu_{j+1} - \nu_j = \alpha\,(\,\nu_j - \nu_{j-1}\,) \qquad (j = 1,\,\ldots,\,N-1)\,,$$

where $\alpha = 1.1$ and $\nu_1 = 10^{-4}$. Coarser frequency grids are constructed from the finest grid. For simulations using $N = 2$, 4, 8, 16, 32 groups, the coarse grid boundaries are given by

$$\nu_0 < \nu_{64/N} < \nu_{2\cdot 64/N} < \cdots < \nu_{N\cdot 64/N}\,.$$

The cube of the "representative frequency" $\mu_j$ is defined as $\mu_1 = (\nu_1/2)^3$, and $\mu_j = (\nu_j\nu_{j-1})^{3/2}$ for $j = 2, \ldots, N$. The emission coefficient $p_j$ is computed using $T_0 = 0.1$, and the "specific heat" $R$ is set to unity.

We refer to the initially localized matter energy problem discussed in section 2 as Problem 1 and to the explicit matter source problem (section 3) as Problem 2. The two problems have similar results, especially for late times, which is not surprising. For the

[5] When the integrand is not in the desirable form, the integrator frequently returns error indicators, of the type "The integral is divergent or slowly convergent" or "The requested accuracy has not been achieved", but does not do so when the desirable form is used.

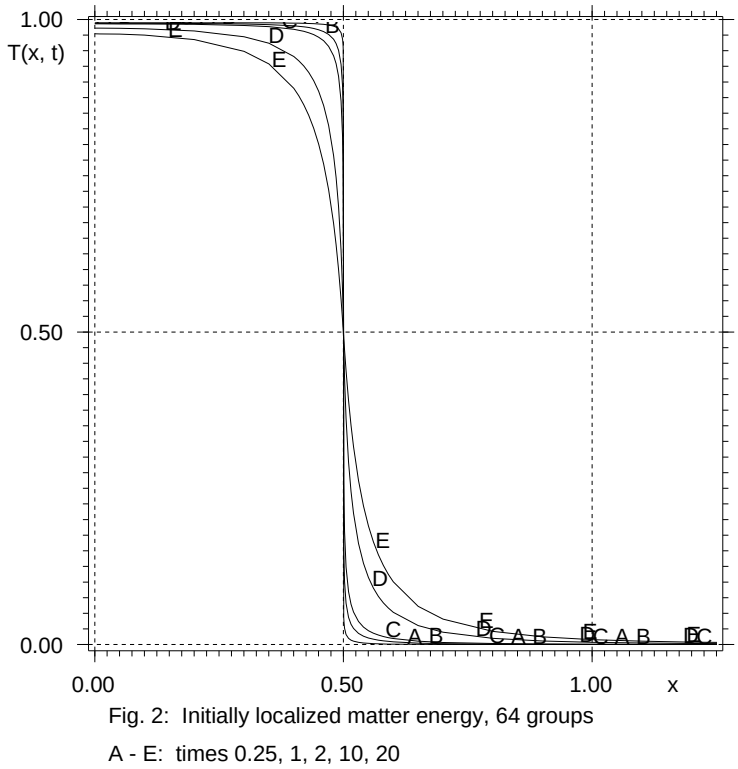


Fig. 2. Problem 1. $T$ vs. $x$ at $t = 0.25$ (curve A), 1.0 (B), 2.0 (C), 10.0 (D), and 20.0 (E); $N = 64$

parameters chosen and for $t \geq t_0$, both problems contain the same energy, cf. (12) and (21). Furthermore, in both problems, the initial energy is put into $T$ in effectively the same position. Only in early times, should we expect much difference since in Problem 2 the energy is continuously sourced for $t \leq t_0$.

Figures 2 and 3 display $T$ and $E_r (= \sum_j w_j)$ vs. $x$ at various times for the case using $N = 64$ groups for Problem 1. Figures 4 and 5 are the corresponding plots for Problem 2. As expected, for larger $t$, the profiles are more diffuse. Although even for $t = 20$, very little energy has been transported beyond $x = 1$. As previously mentioned, the biggest difference between Problems 1 and 2 is at $t = 0.25$ (cf. curves A). Comparing the magnitudes of $T$ $(\approx 1.0)$ and $E_r$ $(\approx 1.0)$ shows that most of the energy is contained in the matter, at least up to $t = 20$.

Next, we focus attention at $t = 2$ (the approximate time when the fields attain their maximum magnitude) and examine how the results converge as the number of groups $N$ is increased. In order to demonstrate convergence, we concentrate on the domain $x \leq 0.5$ and limit the ordinate's range to magnify the distinction for $N \geq 4$. Figures 6 and 7 display $T$ and $E_r$ for Problem 1 while Figs. 8 and 9 pertain to Problem 2. Second order convergence is evident. The $N = 2$ result (curve A, evident only in Figs. 7 and 9) is clearly significantly different from the correct multifrequency result, $N = 64$.

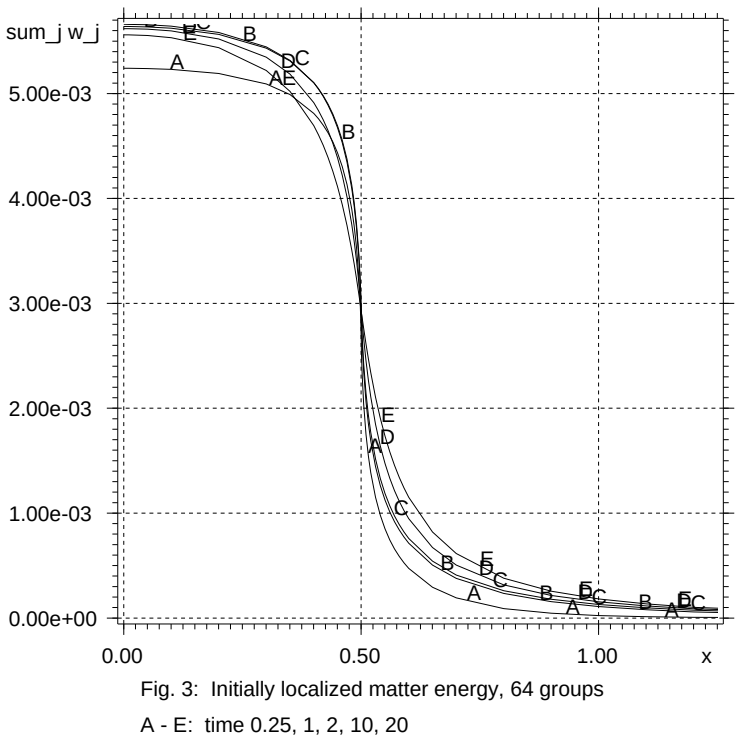


Fig. 3. Problem 1. $E_r$ vs. $x$ at $t = 0.25$ (A), 1.0 (B), 2.0 (C), 10.0 (D), and 20.0 (E); $N = 64$

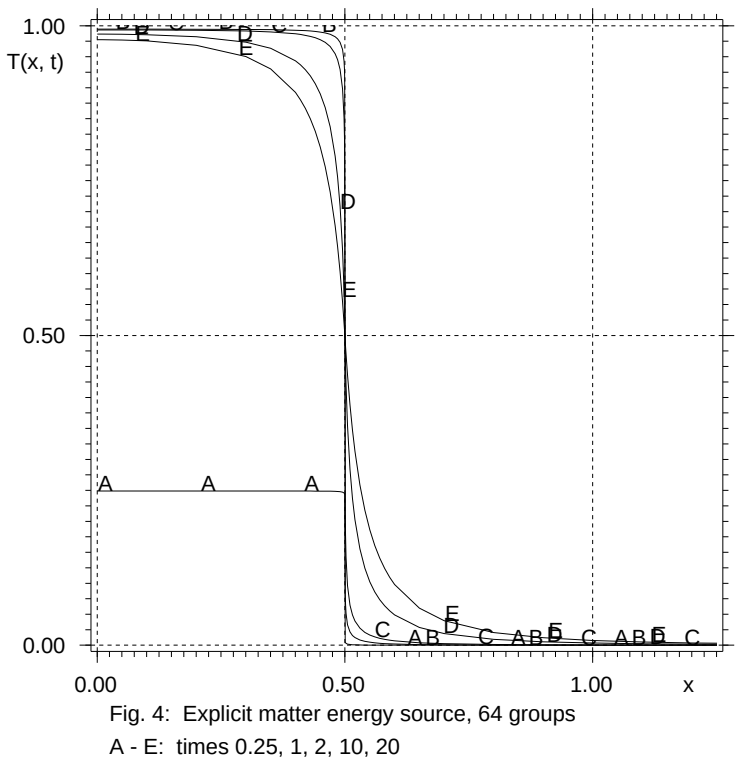


Fig. 4. Problem 2. $T$ vs. $x$ at $t = 0.25$ (A), 1.0 (B), 2.0 (C), 10.0 (D), and 20.0 (E); $N = 64$

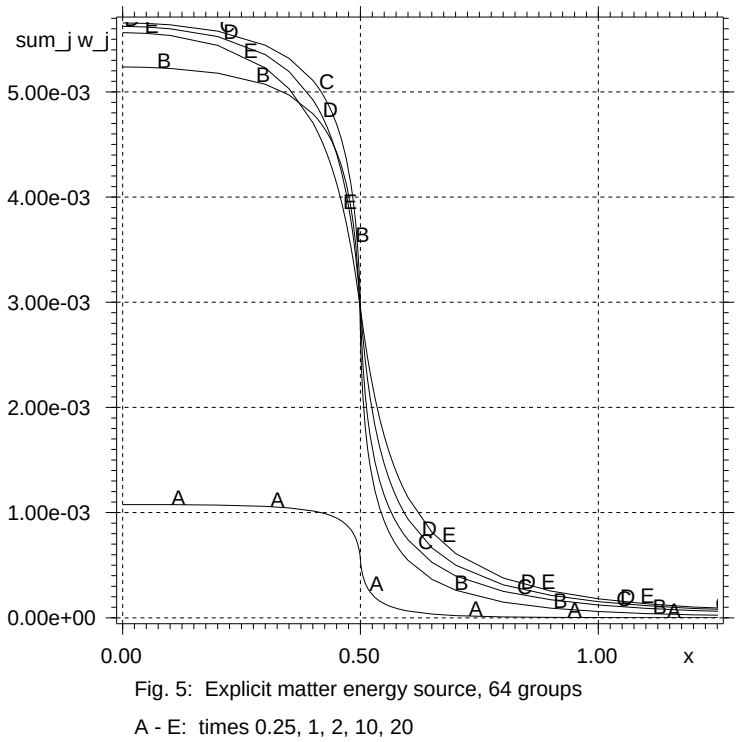


Fig. 5. Problem 2. $E_r$ vs. $x$ at $t = 0.25$ (A), 1.0 (B), 2.0 (C), 10.0 (D), and 20.0 (E); $N = 64$

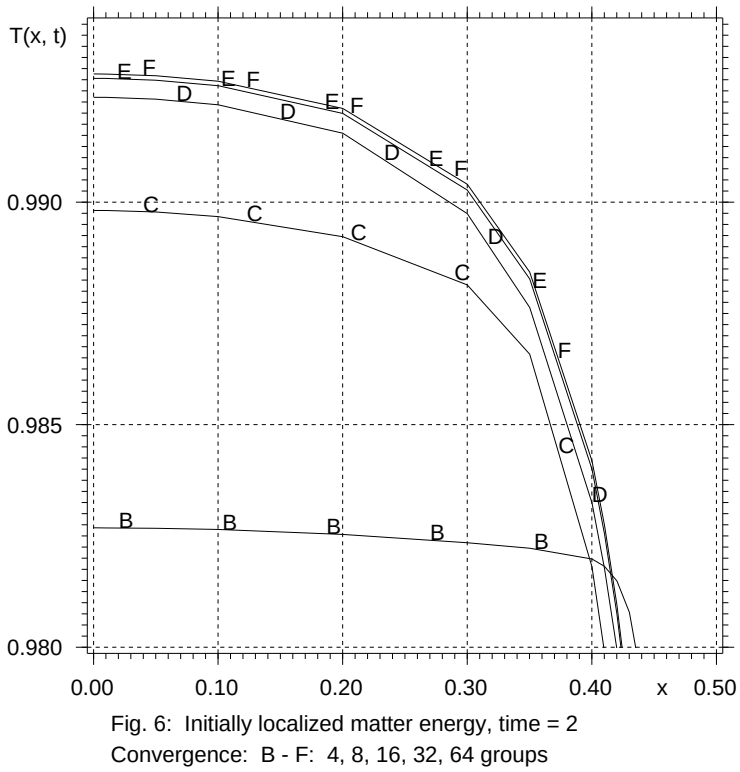


Fig. 6. Problem 1. $T$ vs. $x$ at $t = 2$ for $N = 4$ (curve B), 8 (C), 16 (D), 32 (E), and 64 (F) groups

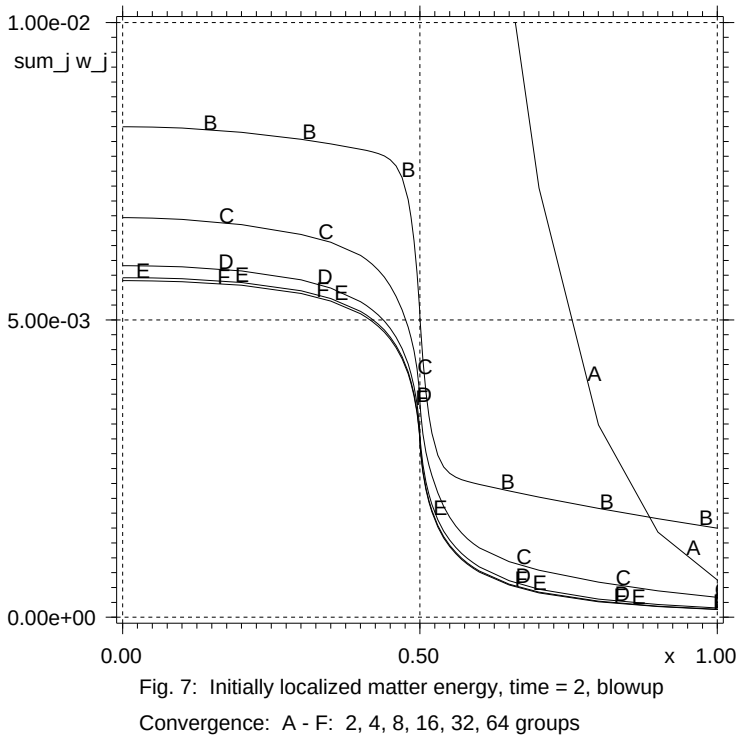


Fig. 7. Problem 1. $E_r$ vs. $x$ at $t = 2$ for $N = 2$ (A), 4 (B), 8 (C), 16 (D), 32 (E), and 64 (F) groups

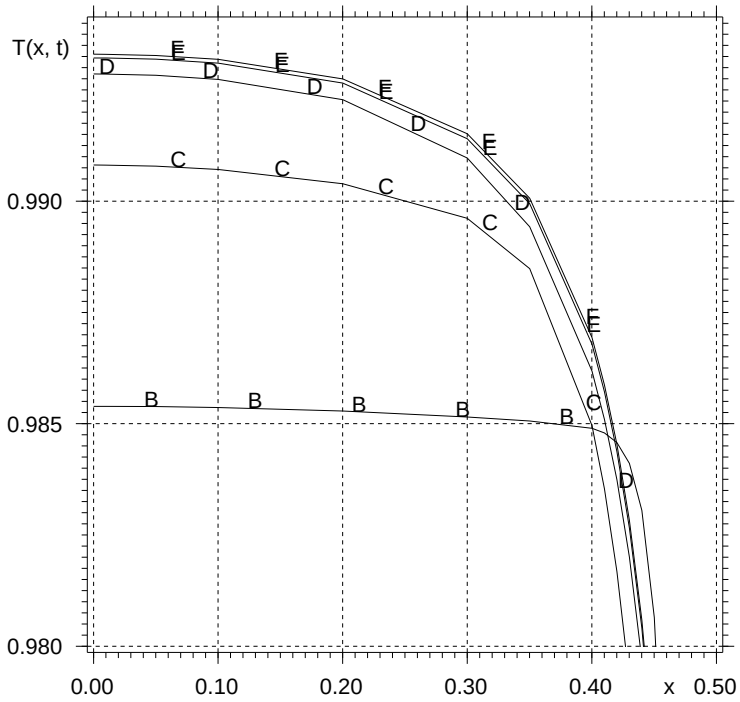


Fig. 8. Problem 2. $T$ vs. $x$ at $t = 2$ for $N = 4$ (B), 8 (C), 16 (D), 32 (E), and 64 (F) groups

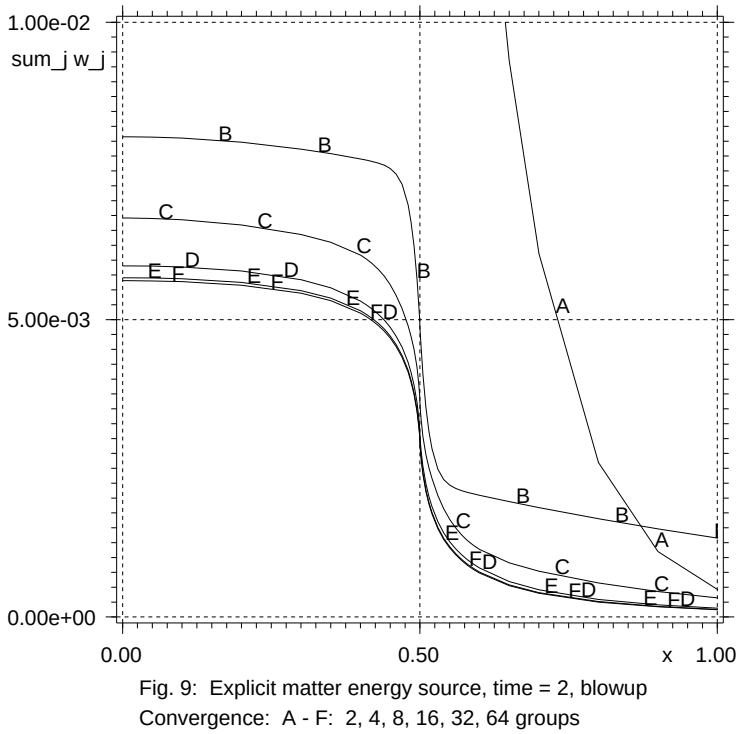


Fig. 9. Problem 2. $E_r$ vs. $x$ at $t = 2$ for $N = 2$ (A), 4 (B), 8 (C), 16 (D), 32 (E), and 64 (F) groups

## 6. Summary

We have presented an exact solution for a linearization of a model, the H&S equations, simulating multigroup radiation diffusion. The model captures the salient effects of the physical equations, viz., an ideal gas equation of state and opacities varying as the inverse cube of the frequency [1]. For ease of analysis, the model assumes that the radiation emission function is given by a Wien (rather than a Planck) distribution. This distinction is not significant; only for low frequencies is there a significant difference between the two.

The H&S equation are nonlinear. Our linearization is equivalent to linearizing the emission function about a fixed temperature $T_0$. Although this is gross simplification, the linearized system retains salient aspects of multifrequency diffusion: high (low) free frequency radiation diffuses quickly (slowly) and absorbs poorly (well).

To conclude, we analyze the emission and absorption terms of the H&S model in order to shed light on the effects of using a Wien rather than a Planck distribution. In (1), these terms are,

$$p_j\, T - w_j/\mu_j \ .$$

Recalling the definitions, the coupling terms for the $j$th group represent

$$\int_{\nu_{j-1}}^{\nu_j} d\nu \, \left( e^{-\nu/T} - u/\nu^3 \right) \ ,$$

where $u$ is the spectral energy density. If the exponential is multiplied by $\nu^3/\nu^3$, the coupling term becomes

$$\int_{\nu_{j-1}}^{\nu_j} d\nu \, (1/\nu^3) \left( \nu^3 \, e^{-\nu/T} - u \right) \ ,$$

and the Wien distribution is obvious. Using a Wien distribution brings a twofold advantage. First, it may be integrated exactly over any frequency width. Second, if the emission term is integrated over all frequencies, one obtains,

$$\int_0^\infty d\nu \, (1/\nu^3) \left( \nu^3 \, e^{-\nu/T} \right) = T = (1/6\,T^3) \, (6\,T^4) \ .$$

The result may be interpreted as the product of the "Planck averaged" opacity $(1/6\,T^3)$ times the integrated emission function $6\,T^4$. Note that the factor 6 approximately 8% less than the equivalent factor $\pi^4/15$ of the normalized Planck function. Lastly, we note that for an opacity model which is proportional to $\nu^{-3}$, the corresponding average for the Planck function does not exist; the integral diverges.

# References

[1] O. H. Hald and A. I. Shestakov, "Stability of stationary solutions of the multifrequency radiation diffusion equation," Lawrence Livermore Natl. Lab. UCRL-JC-148079, (2002), submitted to *SIAM J. Appl. Math.*

[2] A. I. Shestakov, "Solution of the nonlinear multigroup radiation diffusion equation using multigrid and pseudo transient continuation," Lawrence Livermore Natl. Lab. UCRL-JC-148873, (2002), submitted to *J. Comp. Phys.*

[3] B. Su and G. L. Olson, "Non-grey benchmark results for two temperature non-equilibrium radiative transfer," *J. Quant. Spec. Rad. Trans.*, **62** (1999) 279-302

[4] B. Su and G. L. Olson, "An analytical benchmark for non-equilibrium radiative transfer in an isotropically scattering medium,," *Ann. Nucl. Energy*, **24**, 13 (1997) 1035–1055

[5] R. Piessens, et al., *QUADPACK: A Subroutine Package for Automatic Integration*, Springer-Verlag, Berlin (1983). (Source is available from www.netlib.org.)

## Acknowledgment

This work was performed under the auspices of the U.S. Department of Energy by the University of California Lawrence Livermore National Laboratory under contract No. W-7405-ENG-48.

University of California
Lawrence Livermore National Laboratory
Technical Information Department
Livermore, CA 94551